

## Quasitransparent states in the logarithmic chain and nontrivial zeros of the Riemann zeta function

D. S. Citrin<sup>\*</sup>

School of Electrical and Computer Engineering, Georgia Institute of Technology, Atlanta, Georgia 30332-0250, USA



(Received 12 September 2023; accepted 24 July 2024; published 13 August 2024)

The Riemann hypothesis is a major open problem in number theory. It asserts that the nontrivial zeros of the Riemann zeta function  $\zeta(x)$  occur on the critical line, i.e., for  $x = u + iy$  with  $u = \frac{1}{2}$ , in the complex plane. We discuss the physical realization of the zeros of  $\zeta(x)$  on the critical line by means of a 1D nonperiodic lattice with sites at positions  $z_j = d \ln(j + 1)$  ( $j \in \{0, 1, 2, \dots\}$ ) along the  $z$  axis with  $d$  a length and the form factors of the sites modulated by  $(-1)^{j+1} e^{-\alpha z_j}$  with  $\alpha d$  playing the role of  $u$ . On the critical line,  $\alpha d = \frac{1}{2}$ . We find quasitransparent states when  $y = \frac{kd}{2}$  is the imaginary part of a zero of  $\zeta(x)$  on the critical line with  $k$  the wave vector of the particle between sites  $z_j$  and  $z_{j+1}$ .

DOI: [10.1103/PhysRevB.110.L081406](https://doi.org/10.1103/PhysRevB.110.L081406)

The Riemann hypothesis [1]—that the nontrivial zeros [2] of the Riemann zeta function  $\zeta(x)$  lie on the critical line (CL)  $x = u + iy$  with  $u = \frac{1}{2}$  in the complex plane—is a major open problem in number theory, bearing on the distribution of the prime numbers, and is a component of Hilbert’s eighth unsolved problem [3].  $\zeta(x)$  is also related to range of disparate physical and engineered systems as well as problems in applied mathematics [4–11]. Notably, the statistics of the nontrivial zeros of  $\zeta(x)$  appear to follow the statistics of the eigenvalues of a Gaussian unitary ensemble, described by complex Hermitian matrices with Gauss distributed elements, which has been suggested to indicate a deep connection between  $\zeta(x)$  and the quantum mechanics of classically chaotic systems lacking time-inversion invariance [12–17]. Indeed, the formal similarities have motivated a potential search for a quantum Hamiltonian whose eigenvalues give the nontrivial zeros of  $\zeta(x)$ .

The present work focuses on the realization of a physical system, namely a one-dimensional nonperiodic lattice or chain, in the spirit of other nonperiodic chains, such as the Fibonacci or Thue-Morse chain, whose scattering properties and electronic structure are closely related to  $\zeta(x)$ . The system under consideration does not provide the sought-after Hamiltonian (for one thing, the system we study has only one degree of freedom). Specifically, upon a judicious choice of parameters, the transport properties of the chain can be used to find the nontrivial zeros of  $\zeta(x)$  on the CL. What must be emphasized here is that a simple physical system can provide insight into a fundamental problem in mathematics and, moreover, the system we propose exhibits unusual transport properties in its own right.

While computing the zeros of  $\zeta(x)$  has become a cottage industry [18,19], it has been noted that  $\zeta(x)$  can also be obtained as the spectrum of a logarithmic-time sequence

of Dirac  $\delta$  functions [20]. This suggests physically realizing  $\zeta(x)$  in *space*, instead of time, as a logarithmic chain (LC) to be defined shortly. Since the standard series expression for  $\zeta(x) = \sum_{n=1}^{\infty} n^{-x}$  is not convergent on the CL, a point missed in Ref. [20], we use the Dirichlet eta function, for which  $\eta(x) = (1 - 2^{1-x})\zeta(x)$ . The zeros of  $\eta(x)$  consequently coincide with those of  $\zeta(x)$  provided  $u \neq 1$ . Our main interest is the CL, for which  $u = \alpha d = \frac{1}{2}$ , though other values can also be considered. Our aim again is to *physically realize* the zeros of  $\zeta(x)$  on the CL in the properties of a potentially attainable structure. Namely, we consider a suitably designed LC (to be specified in the next paragraph), and show that the states for which  $\frac{kd}{2}$  is the imaginary part of a zero of  $\zeta(x)$  on the CL are quasitransparent in the sense that the Landauer resistance goes to zero as  $\frac{|\lambda|}{kd} \rightarrow 0$  approximately to fourth order in  $\frac{|\lambda|}{kd}$ , with  $\lambda$  a parameter characterizing the on-site potentials of the LC (see below) and  $k$  the particle’s wave vector between sites where it acts as a free particle, i.e.,  $kd = \sqrt{E}$ , where  $E$  is an energy eigenvalue in dimensionless units. Transparent states, namely those states for which the Landauer resistance goes to zero as chain length becomes infinite, in quasiperiodic lattices have received considerable attention [21–25]. For the LC, we shall see that states connected with the nontrivial zeros of  $\zeta(x)$  on the CL are almost transparent or quasitransparent whereas other states have distinct scaling of the resistance. The underlying mechanism for quasitransparency in the LC is distinct from transparency in other studied quasiperiodic chains. In particular, the spectra of a number of quasiperiodic chains such as Fibonacci, Thue-Morse, and Gauss chains [26–29] are singular-continuous yet may support delocalized states [30]. The spectrum of the nonperiodic LC, instead, is continuous, yet exhibits isolated states that are transparent in a limiting sense. We shall see that these quasitransparent states are connected to the vanishing of the LC’s structure factor (SF)  $S(2k)$  at the nontrivial zeros of  $\zeta(x)$ .

We start with the SF  $S(k)$  assuming form factor  $(-1)^{j+1} e^{-\alpha z_j}$  at site  $z_j = d \ln(j + 1)$  ( $j \in \{0, 1, 2, \dots\}$ ) with  $d$  a length (without loss of generality, taken below as 1) and  $\alpha > 0$ , as shown in Fig. 1. Thus, the magnitude of

<sup>\*</sup>Contact author: david.citrin@ece.gatech.edu; also at Georgia Tech-CNRS IRL2958, Georgia Tech-Europe, 2 Rue Marconi, 57070 Metz, France.

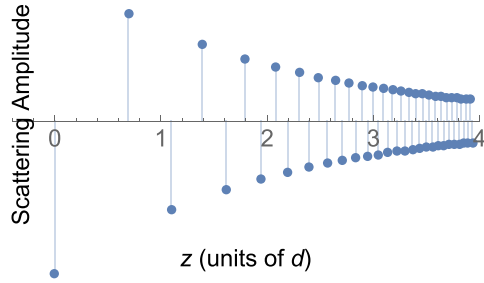


FIG. 1. Schematic diagram showing site positions on  $z$  axis and scattering amplitudes (form factors) as the dots of the LC with sites at  $z = z_j = d \ln(j + 1)$ . The scattering amplitude of site  $j$  is  $(-1)^{j+1} e^{-\alpha z_j}$ . Without loss of generality, we choose  $d = 1$ .

the form factors of successive sites is attenuated by  $\alpha > 0$ , and the signs of the form factors alternate so that the SF yields a result closely related to  $\eta(x)$  as we see just below.  $S(k)$  gives the diffraction pattern in the first Born approximation (neutron, x ray, or optical depending on the relevant field undergoing scattering with  $k$  the wave vector along the chain) and also provides insight into the electronic structure of the chain. The line in the complex plane  $u + iy$  with  $u = \alpha d = \frac{1}{2}$  is the CL, the focus of this study, which, according to the Riemann hypothesis, contains the nontrivial zeros of  $\zeta(x)$ . The LC then is defined by the distribution  $f(z) = \sum_{j=0}^{N-1} (-1)^{j+1} e^{-\alpha z} \delta(z - z_j)$  with  $\alpha > 0$ . The Fourier transform is  $F(k) = \int_{-\infty}^{\infty} dz f(z) e^{-ikz}$  and  $S(k) = |F(k)|^2$ . Explicitly,  $F(k) = \eta(\alpha d + ikd)$  for  $N \rightarrow \infty$  and  $S(k) = |\eta(\alpha d + ikd)|^2$ .

In Fig. 2(a) is shown  $S(k)$  (black) and  $|\zeta(\frac{1}{2} + ikd)|^2$  (red) for  $\alpha d = \frac{1}{2}$ , illustrating that the zeros of  $S(k)$  coincide with those of  $\zeta(x)$  on the CL. Figure 2(b) plots  $|\eta(\frac{1}{8} + ikd)|^2$  (black) and  $8|\eta(\frac{7}{8} + ikd)|^2$  (red); the prefactor 8 is chosen so that all curves have visually comparable scale. Neither of the curves in (b) has a zero. To emphasize,  $S(k)$  achieves zeros coinciding with those of  $\zeta(x)$ , i.e., on the CL, *only* for the value  $\alpha d = \frac{1}{2}$  provided the Riemann hypothesis is correct.

We turn to the solution of the Schrödinger equation in a Kronig-Penney model where the logarithmic sites present Dirac  $\delta$ -function potentials [29]. To a great extent, properties of nonperiodic chains are largely similar whether considered in a tight-binding model or employing continuum models [28]. In the present case, however, we do not pursue a

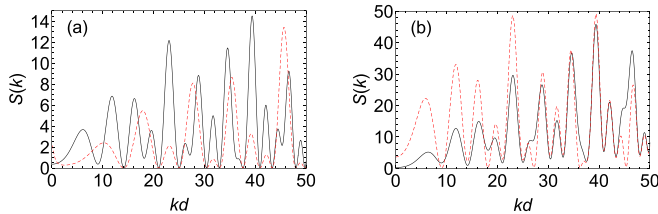


FIG. 2. (a) The structure factor  $S(k) = |\eta(\frac{1}{2} + ikd)|^2$  of the LC (black). Also shown is  $|\zeta(\frac{1}{2} + ikd)|^2$  (red). Both curves exhibit the zeros of  $\zeta(x)$  on the CL. (b)  $|\eta(\frac{1}{8} + ikd)|^2$  (black) and  $8|\eta(\frac{7}{8} + ikd)|^2$  (red) evaluated off the critical line. Neither curve in (b) possesses zeros.

tight-binding approach as, we shall see, we need the actual logarithmic spatial arrangement of sites in the distribution  $f(z)$  to realize  $\eta(x)$ . In the cases of many quasiperiodic chains, tight-binding models preserve the underlying quasiperiodicity. The LC, however, is not a quasiperiodic chain in the sense that the Fibonacci chain and others are. Indeed, we have made desultory attempts at implementing diagonal and off-diagonal tight-binding models for the LC without apparent success.

Continuing with the Kronig-Penney model, a practical LC might have potentials differing from Dirac  $\delta$  functions; however, based on experience with other nonperiodic chains, this is not expected to significantly alter our conclusions. Dirac  $\delta$ -function potentials provide simple numerical means to analyzing the electronic structure of nonperiodic chains.

The Hamiltonian is  $H = -\frac{\hbar^2}{2m^*} \frac{\partial^2}{\partial z^2} + \frac{\hbar^2}{2m^*} \frac{\lambda}{d} f(z)$  with  $m^*$  the effective mass and  $\lambda$  giving the on-site potential strength. For brevity, define the normalized Hamiltonian  $\bar{H} = \frac{2m^*}{\hbar^2} H$  to give the scaled Schrödinger equation  $\bar{H}\psi = \bar{E}\psi$  with  $\bar{E}$  an eigenvalue of  $\bar{H}$  and  $\psi$  the corresponding eigenfunction. Since between sites on the LC the electron acts as a free particle with wave vector  $k$ ,  $kd = \sqrt{\bar{E}}$ .

In Ref. [29], we obtain the transfer matrix  $\mathcal{T}_N$  for an  $N$ -site LC with  $\mathcal{T}_N = Q_N M Q_{N-1} M \cdots M Q_2 M Q_1 M Q_0$ , where  $M = I + i\gamma D$  is the transfer matrix across the  $j$ th site,  $D$  has entries  $D_{1,l} = 1$  and  $D_{2,l} = -1$  for  $l \in \{1, 2\}$ ,  $I$  is the  $2 \times 2$  identity matrix, and  $\gamma = \frac{\lambda}{2kd}$ . The transfer matrix between sites  $j - 1$  and  $j$  is

$$Q_j = \begin{bmatrix} \exp[-ik(z_j - z_{j-1})] & 0 \\ 0 & \exp[ik(z_j - z_{j-1})] \end{bmatrix}. \quad (1)$$

$\mathcal{T}_N$  can be expanded as  $\mathcal{T}_N = \sum_{n=0}^{N-1} (i\gamma)^n T_n$  with

$$T_n = \sum_{p > p' > p'' > \dots > p^{(n-1)} = 0}^{N-1} Q_N Q_{N-1} \cdots Q_{p+1} D Q_p \cdots Q_{p'+1} D Q_{p'} \cdots Q_{p^{(n-1)+1}} D Q_{p^{(n-1)}} \cdots Q_1 Q_0, \quad (2)$$

where  $p^{(j)}$  is  $p$  with  $j$  primes.

We explore conditions for which states are quasitransparent employing the Landauer transport formalism [31,32]. The dimensionless resistance for state  $k$  in an  $N$ -site LC for a given value of  $\alpha d$  is [33,34]  $\rho(N) = \frac{1}{2} (\frac{1}{2} \text{Tr} \mathcal{T}_N^\dagger \mathcal{T}_N - 1)$ . It is useful to define an auxiliary measure of the Landauer re-

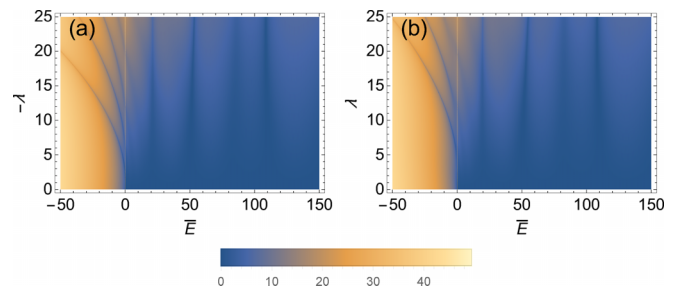


FIG. 3.  $R(N)$  as a function of  $\bar{E} = k^2$  for  $\alpha d = \frac{1}{2}$  on the CL with  $N = 20$ . Dark (light) colors indicate low (high) Landauer resistance as indicated on the legend. The vertical bars occur at the zeros of  $\zeta(x)$  on the CL.

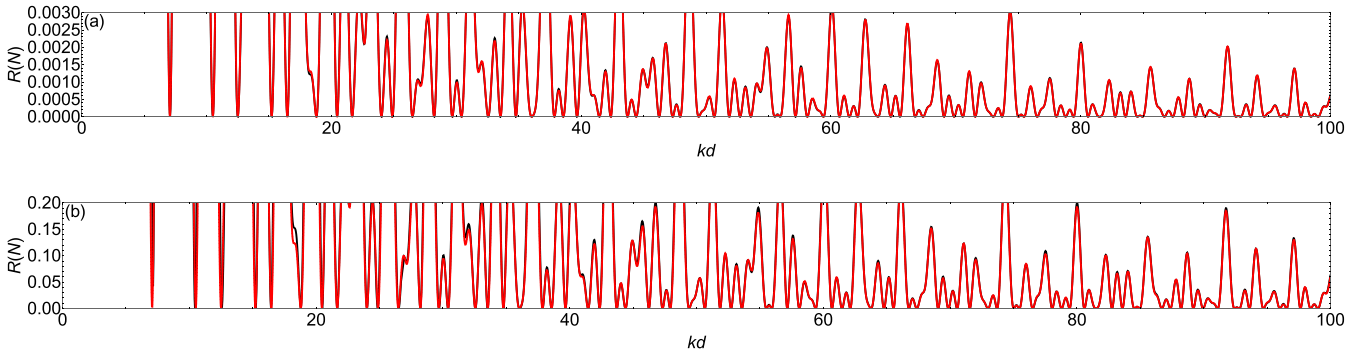


FIG. 4.  $R(N)$  (black) and perturbation-theory expression  $\ln[1 + 2\gamma^2 S(2k)]$  (red) as functions of  $kd$  for (a)  $\lambda = 1$  and (b)  $\lambda = 10$  with  $\alpha d = \frac{1}{2}$  for  $N = 150$ . The black and red curves largely overlap.

sistance  $R(N) = \ln[2\rho(N) + 1] = \ln \frac{1}{2} \text{Tr} \mathcal{T}_N^\dagger \mathcal{T}_N$ . Based on the above [35], we expand  $\text{Tr} \mathcal{T}_N^\dagger \mathcal{T}_N$  to second order in  $\gamma$  to give  $R(N) \approx \ln[1 + 2\gamma^2 S(2k)]$ . Thus,  $R(N)$  will be very small at zeros of  $S(2k)$  giving rise to quasitransparency. The 2 in the argument of the SF is connected to the momentum transfer in an elastic scattering process.

Figure 3 shows  $R(N)$  as a function of  $\bar{E} = k^2$  and  $\lambda$  for  $\alpha d = \frac{1}{2}$ . The vertical bands are at zeros of  $\zeta(x)$  on the CL, though the picture becomes more complex at higher  $|\lambda|$ . While Fig. 3 provides a global view of  $R(N)$ , for quantitative purposes, we show in Fig. 4  $R(N)$  (black) and the perturbation-theory expression  $\ln[1 + 2\gamma^2 S(2k)]$  (red) as functions of  $kd$  with  $\alpha d = \frac{1}{2}$  for (a)  $\lambda = 1$  and (b)  $\lambda = 10$  all for  $N = 150$ . We note that the respective red and black curves almost entirely overlap, indicating the perturbative expression is accurate when  $\frac{|\lambda|}{kd} \ll 1$ . In fact, the leading correction to  $R(N)$  is  $O(\lambda^2)$  unless  $S(2k) = 0$ . In that case, the leading correction is  $O(\lambda^3)$ ; however, due to the alternating signs of the form factor, odd-order terms are small, so in practice the most significant correction is  $O(\lambda^4)$  at zeros of  $\zeta(x)$  on the CL. This is what we call *quasitransparency*.

In Fig. 5 is plotted  $R(N)$  (black) and perturbation-theory expression  $\ln[1 + 2\gamma^2 S(2k)]$  (orange) as functions of  $N$  for  $\lambda = 1$  and  $\alpha d = \frac{1}{2}$  for (a)  $kd/2 = y_{21}$ , (b)  $\frac{y_{21} + y_{22}}{2}$ , (c)  $y_{22}$ , (d)  $\frac{y_{22} + y_{23}}{2}$ , (e)  $y_{23}$ , (f)  $\frac{y_{23} + y_{24}}{2}$ , (g)  $y_{24}$ , and (h)  $\frac{y_{24} + y_{25}}{2}$  with  $y_n$  the

imaginary part of the  $n$ th zero of  $\zeta(x)$  on the CL.  $R(N)$  at the zeros on the CL have numerical values far less than those off the zeros. The behaviors of  $R(N)$  at the zeros on the CL and off the zeros are clearly distinct. In the former case,  $R(N) \approx 0$ , while in the latter,  $R(N) \rightarrow \text{constant} \neq 0$ . The former is an example of a quasitransparent state, viz., a state for which  $R(N) \approx 0$ . We mention in passing that for  $kd/2$  in Fig. 5, panels (b), (d), (f), and (h), which do not correspond to zeros of  $\zeta(x)$ , the curious scaling of  $R(N)$ , i.e., to a constant rather than exponential (localized state) or power law (critical state), is due to the logarithmic spatial nature of the LC, the alternating sign of the scattering amplitudes, and their exponential falloff. As  $N$  increases at a fixed  $k$ , the sites of the LC play a decreasing average in scattering a propagating wave function on the LC.

In Fig. 6 we plot  $R(N)$  for  $N = 1000$  on the CL for the same values of  $kd$  as in Fig. 5 as functions of  $\lambda$ . Note that for cases where  $kd/2 = y_n$ , the state is approximately transparent in  $|\lambda| \lesssim 10$ . Also note the flat bottoms of the curves in the quasitransparent region, in contrast to states for which  $\frac{kd}{2}$  does not correspond to the imaginary part of a zero on the CL. One might think heuristically that the factor  $(-1)^{j+1} e^{-\alpha z_j}$  just balances the decrease in logarithmic cite spacing  $z_{j+1} - z_j$

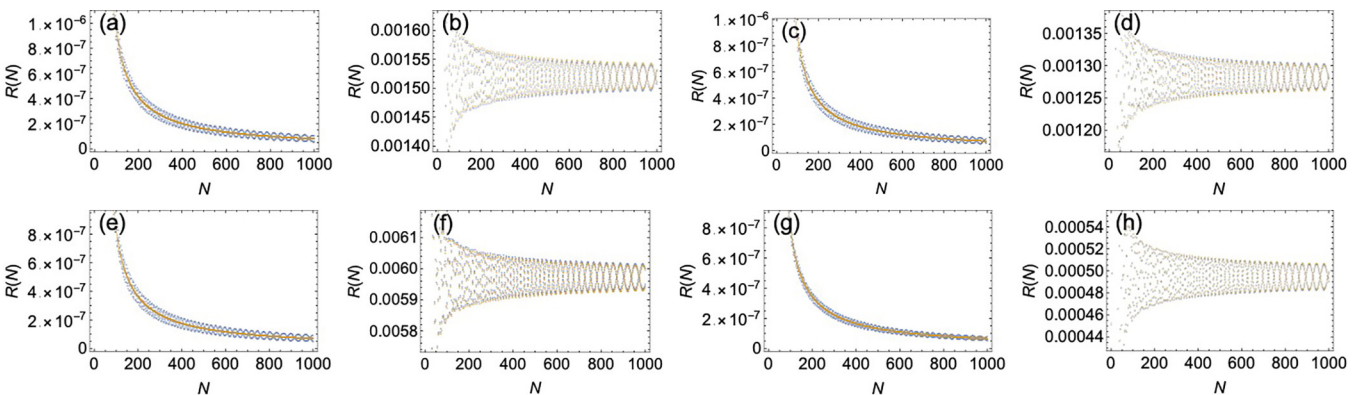


FIG. 5.  $R(N)$  (black) and perturbation-theory expression  $\ln[1 + 2\gamma^2 S(2k)]$  (orange) as functions of  $N$  for  $\lambda = 1$  and  $\alpha d = \frac{1}{2}$  for (a)  $kd/2 = y_{21}$ , (b)  $(y_{21} + y_{22})/2$ , (c)  $y_{22}$ , (d)  $(y_{22} + y_{23})/2$ , (e)  $y_{23}$ , (f)  $(y_{23} + y_{24})/2$ , (g)  $y_{24}$ , and (h)  $(y_{24} + y_{25})/2$ , where  $y_n$  is the imaginary part of the  $n$ th zero of  $\zeta(x)$  on the CL.

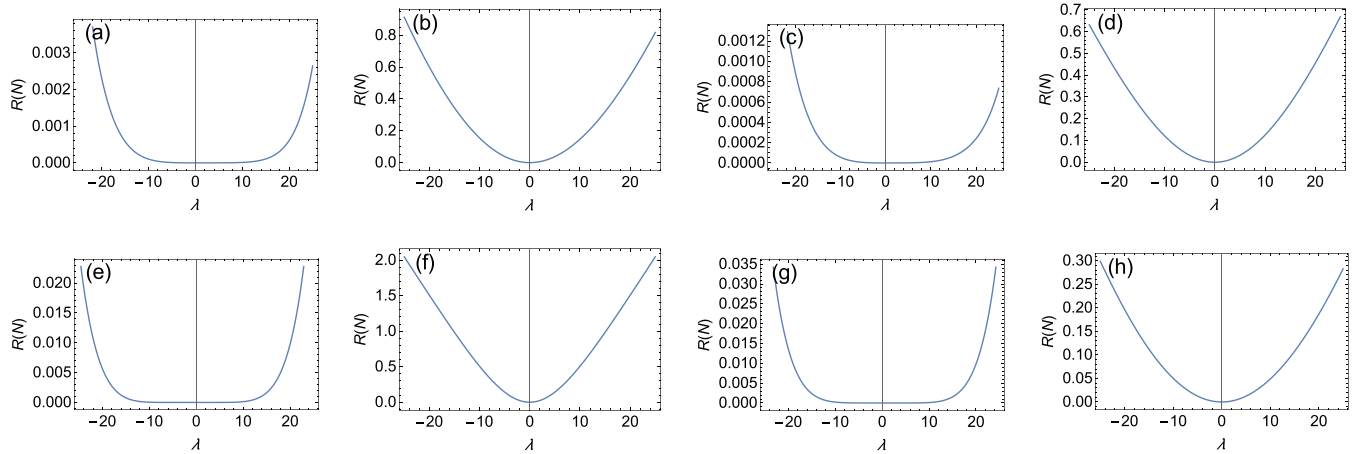


FIG. 6.  $R(N)$  for  $N = 1000$  and  $\alpha d = \frac{1}{2}$  as functions of  $\lambda$  for (a)  $kd/2 = y_{21}$ , (b)  $(y_{21} + y_{22})/2$ , (c)  $y_{22}$ , (d)  $(y_{22} + y_{23})/2$ , (e)  $y_{23}$ , (f)  $(y_{23} + y_{24})/2$ , (g)  $y_{24}$ , and (h)  $(y_{24} + y_{25})/2$ .

with increasing  $j$  for  $\alpha d = \frac{1}{2}$ . That this is not so is proven by the points raised above as well as the fact that states are quasitransparent for neither  $\alpha d > \frac{1}{2}$  nor  $< \frac{1}{2}$ .

We thus identify quasitransparent states, i.e., transparent in the limit  $\lambda \rightarrow 0$ , but approximately transparent for  $\frac{|\lambda|}{kd} \ll 1$ , corresponding to  $y_n = \frac{kd}{2}$  the imaginary part of zeros on the CL by building a LC with  $\alpha d = \frac{1}{2}$ . This suggests that the  $N$ -scaling of the transport properties can be used to identify zeros of  $\zeta(x)$  by the energies of states with low Landauer resistance. The LC can be employed as a filter to pass electrons whose energies correspond to zeros on the CL of  $\zeta(x)$ . Realizing LCs might be possible in suitably designed chain molecules or in semiconductor heterostructures [36]. The existence of

such quasitransparent states in the LC is itself of interest given the focus of much work on localized versus delocalized state in various nonperiodic chains [28]. If a structure could be produced where  $\alpha d$  could be tuned to and away from  $\frac{1}{2}$ , the effects discussed here might be of interest to induce a metal-insulator-like transition in a LC. Moreover, although we do not pursue it here, a grating with an LC amplitude modulation, for example, can produce a diffraction pattern related to  $\zeta(x)$  given by the SF of such a lattice, with the nulls corresponding to the nontrivial zeros on the CL. More broadly, in view of the importance of the Riemann hypothesis, a new physical realization of the nontrivial zeros of  $\zeta(x)$  provides an experimental probe of a central problem in number theory.

- 
- [1] L. Euler, *Commentarii Academiae Scientiarum Petropolitanae* **9**, 160 (1744); B. Riemann, Ueber die Anzahl der Primzahlen unter einer gegebenen Grösse, *Monatsberichte der Berliner Akademie* November (1859).
- [2] Zeros of  $\zeta(s)$ , <https://www.lmfdb.org/zeros/zeta>.
- [3] D. Hilbert, *Mathematische Probleme*, *Göttinger Nachrichten*, 253 (1900); *Archiv der Mathematik und Physik* **3** **1**, 44 (1901); **1**, 213 (1901); *Bull. Am. Math. Soc.* **8**, 437 (1902).
- [4] The Riemann zeta function and tuning, [https://en.xen.wiki/w/The\\_Riemann\\_zeta\\_function\\_and\\_tuning](https://en.xen.wiki/w/The_Riemann_zeta_function_and_tuning).
- [5] A. M. Odlyzko, in *Number Theory* (National Research Council, Washington, DC, 1990), pp. 35–46.
- [6] F. Dyson, *Not. Am. Math. Soc.* **56**, 212 (2009).
- [7] R. A. Hurd and E. V. Jull, *Radio Sci.* **16**, 271 (1981).
- [8] N. A. Nicorovici, R. C. McPhedran, and R. Petit, *Phys. Rev. E* **49**, 4563 (1994).
- [9] D. H. Hoekmann, *IEEE Trans. Geosci. Remote Sensing* **29**, 180 (1991).
- [10] X. Li and M. Anshel, in *Proceedings of the Sixth Annual IEEE SMC Information Assurance Workshop* (IEEE, Piscataway, NJ, 2005), p. 430.
- [11] A. Knauf, *Commun. Math. Phys.* **196**, 703 (1998).
- [12] M. V. Berry, *Lect. Notes Phys.* **263**, 1 (1986).
- [13] J. V. Armitage, in *Number Theory and Dynamical Systems*, edited by M. M. Dodson and J. A. G. Vickers, *London Math. Soc. Lect. Note Ser.* 134 (Cambridge University Press, Cambridge, 1989), pp. 153–172.
- [14] J. P. Keating, in *Quantum Chaos*, edited by G. Casati, I. Guarneri, and U. Smilansky (North-Holland, Amsterdam, 1993), pp. 145–185.
- [15] J. P. Keating, in *Supersymmetry and Trace Formulae: Chaos and Disorder*, edited by J. P. Keating, D. E. Khmelnitskii, and I. V. Lerner (Plenum, New York, 1998), pp. 1–15.
- [16] M. V. Berry and J. P. Keating, *SIAM Rev.* **41**, 236 (1999).
- [17] E. Bogomolny, *Prog. Theor. Phys. Suppl.* **166**, 19 (2007).
- [18] A. M. Odlyzko, *Contemp. Math.* **290**, 139 (2001).
- [19] A. Torres-Hernandez and F. Brambila-Paz, *Math. Stat.* **9**, 309 (2021).
- [20] H. Olkkonen and J. T. Olkkonen, *Open J. Discrete Math.* **1**, 62 (2011).
- [21] E. Maciá, *Phys. Rev. B* **60**, 10032 (1999).
- [22] A. Jagannathan and M. Tarzia, *Eur. Phys. J. B* **93**, 46 (2020).
- [23] V. Sánchez and C. Wang, *Symmetry* **12**, 430 (2020).
- [24] A. Chakrabarti, *Phys. Rev. B* **60**, 10576 (1999).
- [25] V. Sánchez, L. A. Pérez, R. Oviedo-Roa, and C. Wang, *Phys. Rev. B* **64**, 174205 (2001).

- [26] A. Sütő, *J. Stat. Phys.* **56**, 525 (1989); J. Bellissard, B. Iochum, E. Scoppola, and D. Testard, *Commun. Math. Phys.* **125**, 527 (1989).
- [27] J. Bellissard, A. Bovier, and J.-M. Ghez, *Commun. Math. Phys.* **135**, 379 (1991); A. Bovier and J.-M. Ghez, *ibid.* **158**, 45 (1993).
- [28] A. Jagannathan, *Rev. Mod. Phys.* **93**, 045001 (2021).
- [29] D. S. Citrin, *Phys. Rev. B* **107**, 125150 (2023); **107**, 235144 (2023).
- [30] E. Maciá and F. Domínguez-Adame, *Phys. Rev. Lett.* **76**, 2957 (1996).
- [31] B. Sutherland and M. Kohmoto, *Phys. Rev. B* **36**, 5877 (1987).
- [32] B. S. Andereck and E. Abrahams, in *Physics in One Dimension*, edited by J. Bernasconi and T. Schneider (Springer, New York, 1981), pp. 317–320.
- [33] M. Kohmoto, *Phys. Rev. B* **34**, 5043 (1986).
- [34] E. Maciá, *International Scholarly Research Notices* **2014**, 165943 (2014).
- [35] D. S. Citrin, *Phys. Lett. A* **480**, 128978 (2023).
- [36] R. Merlin, *IEEE J. Quantum Electron.* **24**, 1791 (1988).